RNA (1998), *4*:777–788. Cambridge University Press. Printed in the USA.

The P15-loop of *Escherichia coli* RNase P RNA is an autonomous divalent metal ion binding domain

JOANNA KUFEL[1] and LEIF A. KIRSEBOM
Department of Microbiology, Biomedical Center, 751 23 Uppsala, Sweden

ABSTRACT

We have studied the structure and divalent metal ion binding of a domain of the ribozyme RNase P RNA that is involved in base pairing with its substrate. Our data suggest that the folding of this internal loop, the P15-loop, is similar irrespective of whether it is part of the full-length ribozyme or part of a model RNA molecule. We also conclude that this element constitutes an autonomous divalent metal ion binding domain of RNase P RNA and our data suggest that certain specific chemical groups within the P15-loop participate in coordination of divalent metal ions. Substitutions of the Sp- and Rp-oxygens with sulfur at a specific position in this loop result in a 2.5–5-fold less active ribozyme, suggesting that Mg^{2+} binding at this position contributes to function. Our findings strengthen the concept that small RNA building blocks remain basically unchanged when removed from their structural context and thus can be used as models for studies of their potential function and structure within native RNA molecules.

Keywords: metal ion coordination; RNase P; ribozyme

INTRODUCTION

RNase P is a ubiquitous endoribonuclease responsible for generating tRNA molecules with matured 5′ termini. In Bacteria, the catalytic activity of this ribonucleoprotein is conferred by its RNA subunit (Guerrier-Takada et al., 1983; Altman et al., 1995; Kirsebom, 1995; Pace & Brown, 1995). This RNA is able to correctly cleave a number of substrates in vitro in the absence of the protein subunit. This reaction requires divalent metal ions and, among these, Mg^{2+} promotes cleavage most efficiently. A well-conserved GGU-motif in *Escherichia coli* RNase P RNA (designated M1 RNA) base pairs with the 3′-terminal RCCA sequence (interacting residues underlined) of a tRNA precursor (Kirsebom & Svärd, 1994; Oh & Pace, 1994; Svärd et al., 1996; Tallsjö et al., 1996). This motif is part of an internal loop, the P15-loop, located between helices P15 and P16, according to the nomenclature of Brown (1996). Divalent metal ions, including Mg^{2+} and Pb^{2+}, promote spontaneous cleavage of M1 RNA at specific positions (Kazakov & Altman, 1991; Zito et al., 1993; Ciesiolka et al., 1994; see Fig. 1). Two of these cleavage sites are located within the P15-loop, and it has been discussed that the Mg^{2+}-ion(s) generating this cleavage is important for the function of M1 RNA (Kazakov & Altman, 1991; Kirsebom & Svärd, 1993). The three-dimensional structure of a 31-mer RNA molecule harboring the P15-loop of M1 RNA was recently determined by NMR spectroscopy (Glemarec et al., 1996). To investigate whether the folding of the P15-loop in the contexts of M1 RNA and the 31-mer RNA is similar, we probed the structure of various 31-mer RNA derivatives chemically and enzymatically as well as by divalent metal ion cleavage. From these data, together with previous data using intact M1 RNA, we conclude that the structure of the P15-loop in the small RNA is similar to the structure of this region in M1 RNA. Additionally, specific chemical groups in the P15-loop involved in divalent metal ion coordination were identified by studying Mg^{2+}- and Pb^{2+}-induced cleavage of various derivatives of this 31-mer RNA carrying modifications at specific positions. Studies using full-length M1 RNA where Rp- and Sp-oxygens at a specific position in the P15-loop were substituted with phosphorothioates suggest that Mg^{2+}-coordination at this site is indeed im-

Reprint requests to: Leif A. Kirsebom, Department of Microbiology, Box 581, Biomedical Center, 751 23 Uppsala, Sweden; e-mail: leif.kirsebom@mikrobio.uu.se.

[1]Present address: Institute of Cell and Molecular Biology, University of Edinburgh, S-Swann Building, King's Buildings, Edinburgh EH9 3JR, United Kingdom.

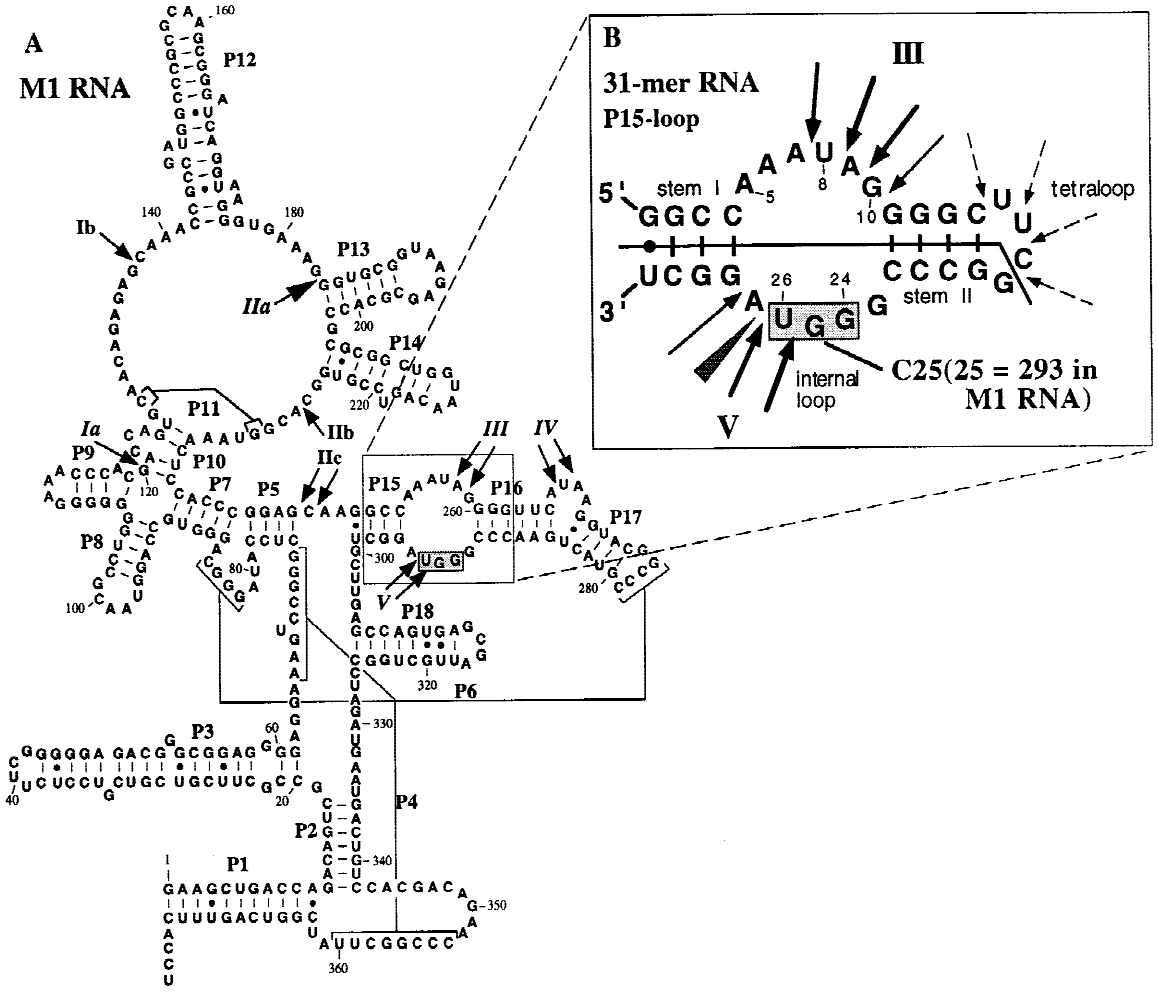

FIGURE 1. A: Secondary structure model of *E. coli* RNase P RNA (M1 RNA) according to Brown (1996). Specific Pb^{2+}-induced cleavage sites are indicated by arrows and roman numerals, whereas Mg^{2+}-induced cleavage sites are shown by numerals in italics. Shaded nucleotides represent residues that base pair with the 3′-terminal RCCA-motif of a precursor (Kirsebom & Svärd, 1994). **B:** Schematic illustration of the 31-mer RNA carrying the P15-loop of M1 RNA. Arrows indicate Mg^{2+}- and Pb^{2+}-induced cleavage, with dashed arrows for unique Pb^{2+}- induced cleavage sites in the tertaloop. A line dividing the molecule into two halves indicates the site where the two RNA fragments were ligated to generate "semi-specifically" substituted molecules containing modifications in either of the halves (see Materials and Methods). Grey box indicates cleavage of RNA–DNA hybrid by RNase H. Substitutions at positions 8, 9, and 25 were made as indicated (U8, A9, and G25 correspond to U257, A258, and G293, respectively, in full-size M1 RNA). Shaded nucleotides depict residues in intact M1 RNA involved in base pairing with the substrate.

portant for function. These data are discussed in view of the three-dimensional structure of the 31-mer RNA and function of M1 RNA.

RESULTS AND DISCUSSION

The P15-loop is an autonomous divalent metal ion binding domain

To investigate whether the P15-loop within the 31-mer RNA forms a structure sufficient to coordinate divalent metal ions, we decided to analyze Mg^{2+}- and Pb^{2+}-induced cleavage of this short RNA and compare it with the divalent metal ion cleavage pattern of full-length M1 RNA. The results are presented in Figure 2A (data only shown for cleavage with Pb^{2+} and Mg^{2+}, however, similar results were obtained using Mn^{2+} or Ca^{2+}) and summarized in Figure 1B (unless stated otherwise, numbering throughout this study refers to the numbering of the 31-mer RNA in Fig. 1B). Both divalent metal ions promote cleavage at overlapping positions: 3′ of A7, U8, and A9 in the upper part of the internal loop and 3′ of G25 and U26 in the lower part of the loop. These cleavage sites correspond to sites III and V in intact M1 RNA (Kazakov & Altman, 1991; Zito et al., 1993; Ciesiolka et al., 1994; Fig. 1; data not shown). Cleavage sites ob-

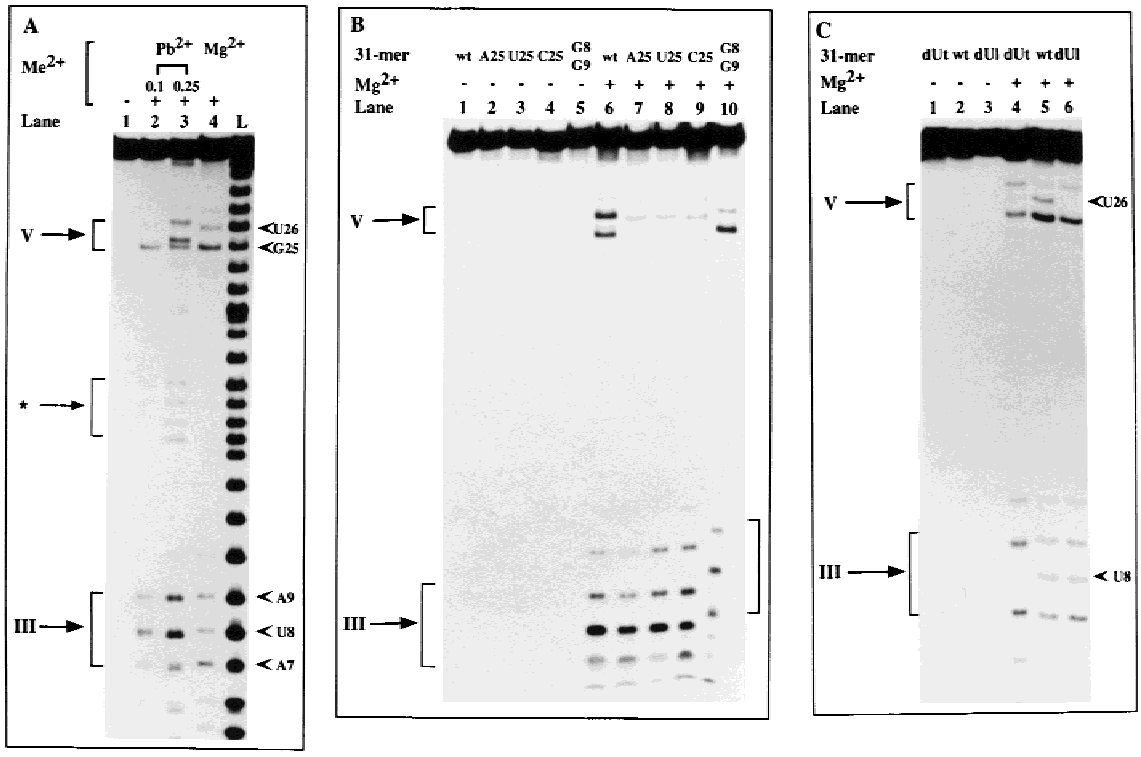

FIGURE 2. Metal ion-induced cleavage of various 5′ end-labeled derivatives of the 31-mer RNA used in this study. Cleavage sites III and V are indicated with arrows (see Fig. 1B). Arrowheads indicate relevant positions. Experiments were performed as outlined in Materials and Methods and the cleavage products and uncleaved RNA were separated on 20% denaturing polyacrylamide gels. **A:** Lead(II)- and magnesium(II)-induced cleavage of wild-type (wt) 31-mer RNA. $Pb(OAc)_2$ was added to a final concentration of 0.1 mM and 0.25 mM, $MgCl_2$ was added to a final concentration of 10 mM, as indicated. L represents partial alkaline ladder using 5′ end-labeled 31-mer RNA. Additional Pb^{2+} cleavage sites observed in the tetraloop are indicated with an asterisk. **B:** Magnesium(II)-induced cleavage of wild-type (wt) 31-mer RNA (lanes 1 and 6) and of various derivatives mutated at position 25 (A25, lanes 2 and 7; U25, lanes 3 and 8; C25, lanes 4 and 9) or at positions 8 and 9 (G8G9, lanes 5 and 10). $MgCl_2$ was added to a final concentration of 10 mM as indicated. **C:** Magnesium(II)-induced cleavage of wild-type (wt) 31-mer RNA (lanes 2 and 5) and its derivatives substituted with deoxyU in the lower (dUl; lanes 3 and 6) and upper (dUt; lanes 1 and 4) half of the molecule. $MgCl_2$ was added to a final concentration of 10 mM as indicated.

served 3′ of G25 and U26 are in agreement with binding of metal ion(s) in this region as predicted by NMR studies (Glemarec et al., 1996). In the presence of higher concentrations of Pb^{2+}, additional cleavage sites in the tetraloop were observed (e.g., see Fig. 2A, lane 3). The absence of Mg^{2+}-induced cleavage at these sites does not exclude the possibility of a Mg^{2+} ion(s) being present in the vicinity of this region. In fact, the NMR data suggest a Mg^{2+} binding site in the vicinity of G18 (Glemarec et al., 1996), but this (or these) Mg^{2+} does not promote cleavage. In any case, this metal ion binding site is not relevant for the function of M1 RNA, because the tetraloop is not present in M1 RNA at this position. In conclusion, this short RNA molecule represents an autonomous divalent metal ion binding domain of M1 RNA. This finding suggests that the P15-loop within the 31-mer forms a structure that is comparable to that of the equivalent loop in full-length M1 RNA.

The P15-loop within the 31-mer RNA is a model molecule for the corresponding region in M1 RNA

Substitutions of a guanosine to adenosine and cytosine at position 293 in M1 RNA reduced Pb^{2+}-induced cleavage at site V, whereas cleavage at site III was not affected (Kufel & Kirsebom, 1996; see Fig. 1; and data not shown). If the structure of the P15-loop in the 31-mer RNA is the same as in the full-length M1 RNA, it is expected that substitutions of G25 (corresponding to position 293 in M1 RNA, see Fig. 1B) would affect divalent metal ion cleavage 3′ of this position. As shown in Figure 2B, cleavage with Mg^{2+} at this site (V) was clearly decreased when the mutated derivatives of the 31-mer RNA were used, whereas cleavage at site III was not altered. Identical results were also observed in the case of cleavage with Pb^{2+} (data not shown). Similar analogy between the 31-mer RNA and M1 RNA

was observed in the case of changes in the upper part of the P15-loop. The main Mg^{2+}-induced cleavage, particularly at site III, was clearly shifted in the case of the mutant 31-mer RNA carrying substitutions at positions 8 and 9 (corresponding to residues 257 and 258 in M1 RNA) to two guanosines when compared to the wild-type (Fig. 2B). This is consistent with a changed metal ion cleavage pattern observed previously for mutant $M1_{G257G258}$ RNA (Kufel & Kirsebom, 1996). We conclude that the 31-mer RNA is folded in a similar way as the corresponding P15-loop in the intact M1 RNA, generating a binding pocket(s) for divalent metal ion(s).

The structural analogy between the P15-loop confined within both M1 RNA and the 31-mer RNA is further supported by chemical and enzymatic probing of the 31-mer RNA (data not shown). Generally, these results are in agreement with structural probing performed on intact M1 RNA (Guerrier-Takada & Altman, 1984; Shiraishi & Shimura, 1988; Knap et al., 1990; LaGrandeur et al., 1994; data not shown) as well as with the NMR-based structure of the 31-mer RNA (Glemarec et al., 1996; Fig. 6A). The enzymatic probing data of the 31-mer RNA, using RNase T1, RNase T2, and RNase V1, support the evidence for the helical stem structures, stem I and II (Fig. 1B), as well as for a more flexible internal loop. Likewise, chemical probing of the base pairing positions [N3-C, N3-U, and N1-A using DMS and N3-U and N1-G using CMCT (Ehresmann et al., 1987)] is consistent with the NMR structure. Furthermore, probing the N7 positions of guanosines with DMS revealed that all of them were modified, suggesting that these were not involved in tertiary interactions. Probing with DEPC gave similar results for the N7 positions of adenines with the exception that the N7 position of A5 was only partially modified. This suggests that this particular group is less accessible to chemical modification, probably due to base stacking or to not being exposed on the surface of the molecule.

The metal ion cleavage pattern of the 31-mer RNA derivatives carrying changes at position 25 suggests that either a specific chemical group present on G25 is required for metal ion coordination in the vicinity of this position or that its substitution imposes a structural rearrangement of the neighboring nucleotides such that a metal ion(s) is bound differently. Structural probing of the 31-mer RNA mutants (A25 and G8G9; data not shown) using DMS and DEPC shows that there are no significant changes in the accessibility of N7 groups of purines, which indicates that the structures of the mutant variants are not significantly different compared to the structure of the wild-type molecule. However, we cannot exclude that local structural alterations that are not detectable by structural probing could affect metal ion coordination in the loop.

Specific groups present on the bases have been reported to participate in metal ion binding by RNA. Crystal structures of the hammerhead ribozyme and biochemical studies of the hairpin ribozyme revealed that the N7 position of guanosine is most likely a direct ligand coordinating a crucial divalent cation (Pley et al., 1994; Grasby et al., 1995; Scott et al., 1995, 1996). Crystallographic studies of metal ion binding to yeast $tRNA^{Phe}$ suggest that various groups, e.g., guanosine N7 and O6, can form hydrogen bonds to water ligands of bound magnesium (Jack et al., 1977) or directly coordinate lead (Brown et al., 1985). Furthermore, the crystal structures of a 5S rRNA domain and the P4/P6 RNA domain also demonstrate the importance of guanosine N7 and O6 for metal ion binding. We also note that two neigboring guanosines are involved in metal ion binding in these structures (Cate & Doudna, 1996; Cate et al., 1996, 1997; Correll et al., 1997). This is similar to the situation in the P15-loop. Together with our present findings that all nucleotide changes at position 25 interfere with cleavage by metal ions, this might imply that more than one chemical group of this guanosine is strictly required for cleavage at site V.

The GGU-motif in the lower half of the P15-loop is accessible to base pairing

We also investigated whether the GGU-motif in the lower half of the P15-loop, which in M1 RNA base pairs with the 3′-terminal RCCA sequence of a pre-tRNA (Kirsebom & Svärd, 1994; Svärd et al., 1996; Tallsjö et al., 1996), is accessible for base pairing in the case of the 31-mer RNA. To assess this, an excess (5–50-fold) of a short DNA oligonucleotide, 5′-CACCCA, carrying four nucleotides complementary to G23–U26 (corresponding to G291–U294 in M1 RNA) was hybridized under native conditions to the 31-mer RNA. Subsequent addition of RNase H resulted in cleavage 3′ of U26 (Fig. 3) showing that a DNA–RNA hybrid had been formed. In an analogous experiment using the same DNA oligonucleotide and a mutant version of the 31-mer RNA carrying a G to C change at position 25, no RNase H cleavage was observed. However, when another DNA oligonucleotide (5′-CAGCCA) complementary to the mutant derivative was used, cleavage by RNase H using the C25 version was detected. These findings suggest that G24, G25 (or C25), and U26 are accessible for base pairing, in keeping with similar results obtained using full-length M1 RNA (Kufel & Kirsebom, 1996). The accessibility of these three residues is expected from the NMR-based structure of the 31-mer RNA where they are exposed on the surface of the molecule (Glemarec et al., 1996; Fig. 6A). Upon binding of the DNA oligonucleotide, we also observed that the N7 position of A5 became even less accessible (if at all) to modification with DEPC (data not shown) compared to the modification pattern in the absence of this DNA oligonucleotide. This observation may indicate that formation of the DNA–RNA hybrid is accompanied with a conformational change(s) of the neighboring resi-

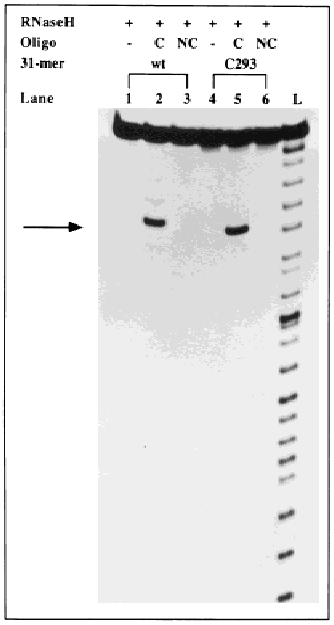

FIGURE 3. RNase H cleavage of RNA–DNA oligonucleotide hybrids. Cleavage reactions were performed as described in Materials and Methods using ^{32}P 5′ end-labeled wild-type (wt) 31-mer RNA (lanes 1–3) or its "C293" derivative (lanes 4–6). A short DNA oligonucleotide (5′-CACCCA or 5′-CAGCCA) was allowed to hybridize to the RNA molecules under native conditions at 33 °C followed by addition of RNase H. Cleavage products and uncleaved RNAs were separated on a 20% denaturing polyacrylamide gel. Arrow indicates the RNase H cleavage observed in the lower half of the internal loop 3′ of U26 [corresponding to U294 in M1 RNA (Kufel & Kirsebom, 1996)]. RNase H and DNA oligonucleotides were added as indicated. L represents partial alkaline ladder of 5′ end-labeled 31-mer RNA. Lanes 1, 4, no DNA oligonucleotide was added; lanes 2, 5, a DNA oligonucleotide, complementary (C) to residues G23–U26 of either wild-type (5′-CACCCA) or the "C293" derivative (5′-CAGCCA) was added; lanes 3, 6, DNA oligonucleotide not fully complementary (NC) to the same region of either wild-type (5′-CAGCCA) or "C293" derivative (5′-CACCCA) was added.

dues in the loop. This would be consistent with our previous hypothesis that the "RCCA–M1 RNA" interaction induces conformational changes within the enzyme–substrate complex, in particular in the P15-loop (Kufel & Kirsebom, 1996). In this context, we also note that a structural model of the P15-loop in complex with the 3′-terminal RCCA-motif of the substrate was presented recently (Easterwood & Harvey, 1997). This model shows similarities with the structure of the P15-loop as determined by NMR (Glemarec et al., 1996; see below), however, there are also obvious differences. Some of these might indeed be due to conformational changes induced by enzyme–substrate complex formation.

Together, these data further strengthen the conclusion that the P15-loop structure is similar within both the 31-mer RNA and M1 RNA. This makes the 31-mer RNA a useful model molecule representing the P15-loop of M1 RNA.

Identification of specific chemical groups of the P15-loop important for divalent metal ion binding

To identify specific chemical groups of the P15-loop important for metal ion-induced cleavage at sites III and V, we generated various derivatives of the 31-mer RNA carrying modified nucleotides at specific positions. These were subsequently subjected to cleavage with Mg^{2+} or Pb^{2+}. The results are shown in Figures 2C and 4A and B.

The P15-loop contains two uridines, U8 and U26. To investigate the roles of 2′-OH groups in metal ion-induced cleavage of the 31-mer RNA, we substituted either of these with deoxyuridine residues by incorporating deoxyuridine into either half of the 31-mer RNA as shown in Figure 1 and outlined in Materials and Methods. Cleavage of these molecules with either Mg^{2+} or Pb^{2+} demonstrated that the 2′-OH groups of U8 and U26, respectively, are essential for cleavage at the respective position (Fig. 2C; only results using Mg^{2+} are shown; however, the same results were obtained in the presence of Pb^{2+}). We also observed that Pb^{2+} cleavage at the minor sites 3′ of U15 and U16 in the tetraloop was abolished (data not shown). These findings support a model for the mechanism of RNA cleavage by metal ions that involves nucleophilic attack of the activated 2′-OH on the adjacent phosphodiester bond (Brown et al., 1985). Based on the findings of these authors, our results might also suggest that, in particular, the catalytic Pb^{2+} are positioned a certain distance (approximately 6 Å) from these 2′-OH groups.

Sulfur is a poor coordination ligand to Mg^{2+}, whereas Pb^{2+} is much more thiophilic (Jaffe & Cohn, 1979). Thus, coordination of Mg^{2+} to the ligands at the sites substituted with sulfur will be significantly decreased, whereas Pb^{2+} would retain or even increase its binding capacity. By following the Mg^{2+} and Pb^{2+} cleavage pattern of Rp-phosphorothioate-modified RNA molecules, it should therefore be possible to identify *pro*-Rp oxygen ligands for both metal ions. Separate 31-mer RNA molecules, each possessing either top or lower half completely substituted with one Rp-phosphorothioate nucleotide analogue (see Fig. 1), were generated and cleaved by Pb^{2+} or Mg^{2+}. The results are presented in Figure 4A and B.

Cleavage by Pb^{2+} of either the thio-U- or the thio-A-substituted RNA molecule revealed a stimulation of cleavage 3′ of U8, G25, and U26 and, less distinctly, 3′ of A7. By contrast, a significant reduction of the magnesium(II)-induced cleavage 3′ of G25 and A7 was observed using both the thio-U- and thio-A-substituted derivatives (Fig. 4A). From the combined data, it is plausible that specific nonbridging *pro*-Rp oxygens in the 31-mer RNA, in particular the *pro*-Rp oxygens 5′ of U26, A27, but most likely also those located 5′ of U8 and A9, are involved in direct coordination of divalent

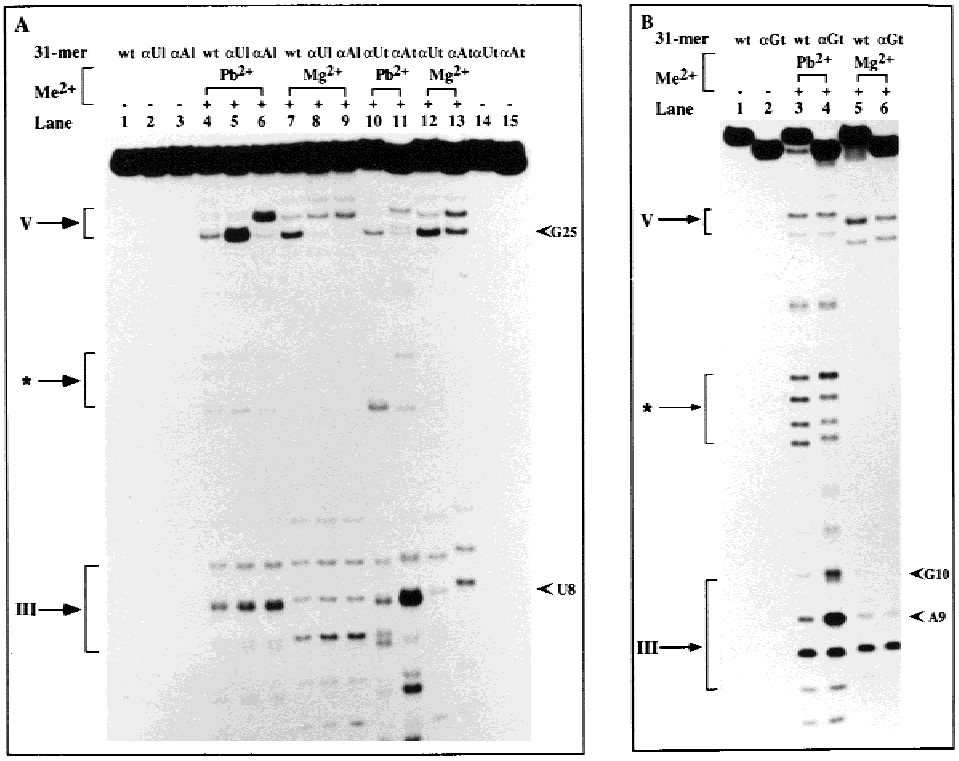

FIGURE 4. Lead(II)- and magnesium(II)-induced cleavage of 5′ end-labeled wild-type and phosphorothioate-substituted 31-mer RNAs. $MgCl_2$ and $Pb(OAc)_2$ were added as indicated to final concentrations of 10 mM and 0.25 mM, respectively. Cleavage sites III and V are indicated with arrows and relevant positions with arrowheads. Additional Pb^{2+} cleavage sites observed in the tetraloop are indicated with an asterisk. **A:** Lanes 1, 4, 7, unmodified 31-mer RNA (wt); lanes 2, 5, 8, 10, 12, 14, RNAs substituted with thioU in the lower (αUl; lanes 2, 5, 8) or upper (αUt; lanes 10, 12, 14) half of the molecule; lanes 3, 6, 9, 11, 13, 15, RNAs substituted with thioA in the lower (αAl; lanes 3, 6, 9) or upper (αAt; lanes 11, 13, 15) half of the molecule. **B:** Lanes 1, 3, 5, unmodified 31-mer RNA (wt); lanes 2, 4, 6, RNAs substituted with thioG in the upper (αGt) half of the molecule.

cations within the P15-loop. [Mg^{2+} or Pb^{2+} coordinated in this way would subsequently result in cleavage 5′ of U26 and U8 (see Fig. 1B).] Metal ions coordinated to these nonbridging oxygens in each half of the molecule are important for metal ion-induced cleavage only in the respective half without affecting cleavage in the other half. We note that the sequence 5′-PuUA is present at both these sites and at another metal ion-induced cleavage site in full-length M1 RNA, site IV (5′-AUA, located in a 4-nt bulge joining two helical stems, see Fig. 1), as well as at metal ion-induced cleavage sites in *Bacillus subtilis* RNase P RNA (Zito et al., 1993) and in a Group I intron (Streicher et al., 1996). Taken together, this might suggest that the 5′-PuUA sequence plays a role in divalent metal ion binding, however, we have to await further experiments using other RNA molecules in order to conclude whether this is the case or not. Furthermore, magnesium(II)-induced cleavage 5′ of, for example, A9 and A27 appears not to be affected by their Rp diastereomers (Fig. 4A). In the proposed mechanism for the hammerhead ribozyme cleavage, direct coordination of Mg^{2+} to *pro*-Rp oxygen at the cleavage site most likely takes place in the transition state of the reaction (Scott et al., 1995, 1996). Our data suggest that this may differ in the case of coordination of metal ions involved in cleavage at these positions in the 31-mer RNA. Thus, another way of coordinating catalytic Mg^{2+} in the vicinity of these particular sites, for example using *pro*-Sp oxygen as a ligand, could be responsible for cleavage at these sites.

Similar analysis of the RNA molecules substituted with thio-G was not conclusive because, although cleavage with Pb^{2+} was stimulated 3′ of A9 and G10, the reduction of the Mg^{2+}-induced cleavage at these sites was less clear (Fig. 4B). The cleavage pattern of the thio-C-substituted RNA did not exhibit any significant differences compared to the natural 31-mer RNA (data not shown). This is expected because no major divalent metal ion cleavage sites are present in the vicinity of the cytidines.

Mg^{2+} binding in the P15-loop contributes to the function of M1 RNA

To investigate whether binding of Mg^{2+} in the P15-loop in M1 RNA is important for catalytic activity, we substituted sulfur for the Rp- and Sp-oxygens between G293

and U294, i.e., divalent metal ion cleavage site V (see Fig. 1A), as outlined in Materials and Methods. As substrate we decided to use a model substrate, pATSer (Fig. 5). Efficient cleavage of this substate is dependent on the "RCCA-M1 RNA" interaction. Cleavage of pATSer by the various M1 RNA derivatives resulted in a 5-fold decrease in efficiency using the Rp-substituted M1 RNA and a 2.5-fold lower activity using the Sp-isomer. This suggests that the function of M1 RNA is indeed affected by a Mg^{2+} coordinated at this position (position V) and, together with the data presented in the previous section, it is likely that the Rp-oxygen 3′ of G293 is directly involved in coordination of a Mg^{2+}-ion. This is supported by modification interference data, which also indicate that the Rp-isomer 3′ of G293 is important for function (Dr. G. Krupp, pers. comm.). Addition of either Mn^{2+}, Cd^{2+}, or Zn^{2+}, however, did not give any increase in cleavage using the Rp- or the Sp-substituted M1 RNA molecules relative to cleavage by wild-type M1 RNA (data not shown). This could indicate that a Mg^{2+} at this position is absolutely required for efficient function and that other ions are coordinated differently at this site, resulting in a less efficient catalyst. That different divalent metal ions may bind to overlapping sites using different ligands is evident from the early studies of the crystal structure of yeast $tRNA^{Phe}$ (Holbrook et al., 1977; Jack et al., 1977; Brown et al., 1985). In this context, we note that an increase in the concentration of Mg^{2+} resulted in only a twofold reduction in the cleavage efficiency for the Rp-substituted M1 RNA (Table 1).

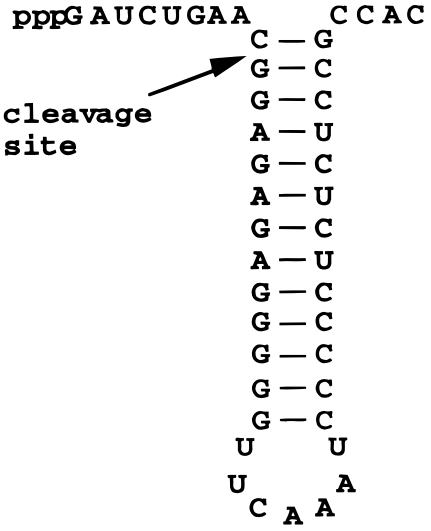

FIGURE 5. An illustration of the secondary structure of pATSer, the model substrate used in this study. The sequence is identical to the 5′ leader, the amino acid acceptor stem, the T-stem, and the T-loop of a precursor to $tRNA^{Ser}$Su1 derived from *E. coli*, with the exception that pATSer only carries an extra C beyond the 3′-terminal CCA-motif and an extra G at the 5′ termini (for details, see Kirsebom & Svärd, 1993). Arrow indicates the cleavage site.

TABLE 1. Relative cleavage of pATSer by the various M1 RNA isomers used in this study.[a]

M1 RNA	40 mM Mg^{2+}	300 mM Mg^{2+}
Wild-type	1	1.8
Rp-isomer	0.19	0.83
Sp-isomer	0.42	0.83

[a]Numbers given represent an average of several independent experiments. The experimental error was ± 22% or less in all cases except cleavage by the Sp-isomer in 300 mM Mg^{2+}, which was ± 28%. For experimental details, see Materials and Methods. Cleavage by wild-type M1 RNA at 40 mM Mg^{2+} was defined as 1 and corresponds to 0.036 pmol substrate cleaved per minute.

We have demonstrated previously that the structural integrity of the P15-loop is important for both cleavage site recognition and divalent metal ion binding in the loop (Kufel & Kirsebom, 1996). The data of Westhof et al. (1996) also suggests that Mg^{2+} plays a significant role in the folding of this domain. Taken together, the function of the Mg^{2+} coordinated at position V in the P15-loop could be either to stabilize the conformation of the P15-loop such that the GGU-motif (residues that base pairs with the 3′-terminal RCCA sequence in the substrate) is in an optimal configuration for base pairing with the substrate and/or its function could merely be to stabilize the "RCCA–M1 RNA" interaction (see above). At present, we cannot completely rule out the possibility that this Mg^{2+} has a role, although indirect, in the chemistry of cleavage. We do not have enough data to explain the role of the Sp-oxygen at this position, but perhaps it contributes to the stabilization of the enzyme–substrate complex.

Correlation of divalent metal ion binding with the NMR structure of the P15-loop

According to our data, two nonbridging oxygens 3′ and 5′ of either of the single uridines in both the top and lower half of the 31-mer RNA are most likely directly participating in coordination of a metal ion involved in cleavage 5′ of each uridine (U8 and U26). In terms of structure, this might indicate a configuration of the 5′-PuUA motif where the central uridine is bulged out, bringing the two *pro*-Rp oxygens close enough to enable them to serve as direct ligands for Mg^{2+}-ions (see above). However, the available structure of the 31-mer RNA is not consistent with this hypothesis (Fig. 6B,C). Here, the two phosphate oxygens mentioned above appear quite distant from each other (approximately 6–7 Å), making it unlikely that they could participate together in coordination of the catalytic metal ion. Additionally, in the NMR-based structure, the 2′-OH groups implied to be involved in cleavage at these two positions are situated considerably distant (>3.5 Å; see Fig. 6B,C) from the target phosphorus atom. Similarly,

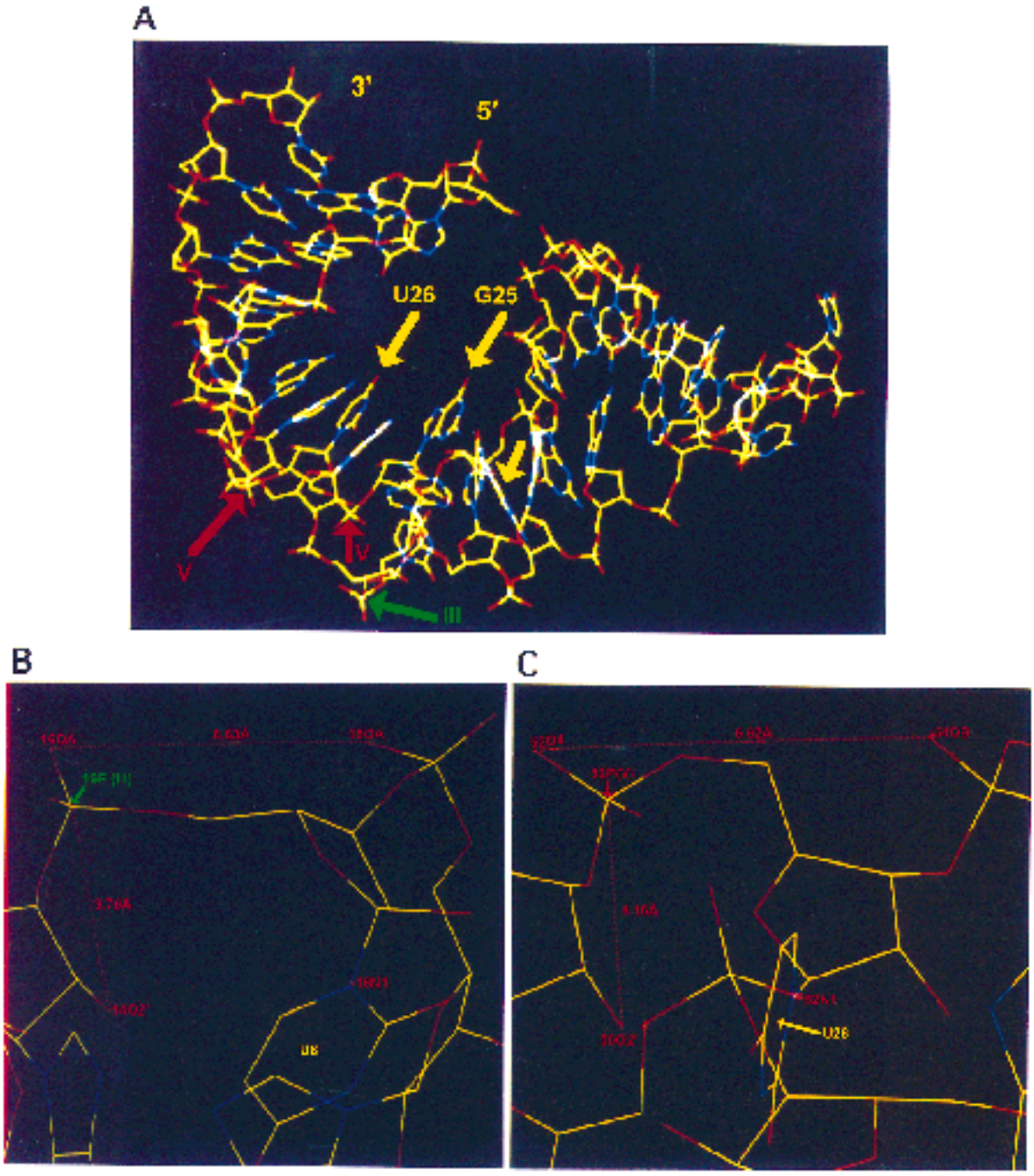

FIGURE 6. A: Representaion of one of several different structures of the 31-mer RNA based on NMR data (Glemarec et al., 1996). Arrows indicate residues of M1 RNA involved in base pairing with the 3′-terminal RCCA of the precursor (yellow arrows) and main divalent metal ion-induced cleavage at sites III (3′ of U8; green arrow) and V (3′ of G25 and U26; red arrows). **B,C:** Representation of the local environment in the vicinity of two Mg^{2+}-induced cleavage sites, III and V (5′ of U8 and U26). Distances between the two respective *pro*-Rp oxygens suggested to be involved in direct coordination of divalent metal ions responsible for cleavage at these sites, and between the attacked phosphorus atom and potentially attacking 2′-OH, are given in Å. **B:** Local structure around U8. The N1 group of U8 (16 N1), *pro*-Rp oxygens of U8 (16 OA) and of A9 (18 OA), target phosphorus of U8 (16 P), and 2′ OH of A7 (14 O2′), implied in the attack on the aforementioned phosphorus atom, are indicated. **C:** Local structure around U26. The N1 group of U26 (52 N1), *pro*-Rp oxygens of U26 (52 OA) and of A27 (54 OB), target phosphorus of U26 (52 P), and 2′ OH of G25 (50 O2′), implied in the attack on the aforementioned phosphorus atom, are indicated.

in the crystallographic structure of the hammerhead ribozyme, the active site is not in the conformation that would support the proposed cleavage mechanism (Pley et al., 1994; Scott et al., 1995). Recent studies revealed that a conformational change in the region of the cleavage site occurred upon cleavage in order to achieve the proposed transition state (Scott et al., 1996; Simorre et al., 1997). Thus, a similar conformational change might occur prior to cleavage 5′ of U8 and U26 in the 31-mer RNA. Further, magnesium-dependent global folding rearrangements were proposed to take place in the case of the hammerhead ribozyme (Bassi et al., 1996). We note that the NMR experiments using the 31-mer RNA were conducted in the absence of Mg^{2+}. It is therefore not excluded that addition of divalent cations may stabilize and/or alter the conformation of the P15-loop. Clearly, further studies have to be performed to understand the biochemical data in terms of structure.

The biochemical data, presented in this study concerning metal ion coordination by specific nonbridging *pro*-Rp oxygens as well as direct participation in catalysis of the 2′-OH groups adjacent to the attacked phoshodiester bond, can be used to model the position of the Mg^{2+} ions in the three-dimensional structure of the P15-loop (Glemarec et al., 1996). This could serve as an approximation of the relative positioning of Mg^{2+} in the P15-loop in full-length M1 RNA (Fig. 6B,C). Such information is essential for designing experiments aimed at elucidating the structural requirements of metal ion coordination within RNase P RNA in particular and RNA in general.

Other structural investigations of RNA molecules, the loop E of eukaryotic 5S rRNA, an ribonuclease III processing signal from bacteriophage T7, a splice leader RNA 1 of *Caenorhabditis elegans*, and the P4/P6 domain of a Group I intron (Wimberly et al., 1993; Schweisguth et al., 1994; Greenbaum et al., 1995; Cate et al., 1996; Xu et al., 1996; Correll et al., 1997), which represent functionally important elements of larger molecules, strengthen the concept that small RNA building blocks remain basically unchanged when taken from their structural context. Together with our present data, this demonstrates the advantage of dissecting a large RNA molecule into small domains and using them as model systems for studies of their potential functional and structural significance within the native molecules.

MATERIALS AND METHODS

Preparation of RNA substrates

The different gene constructs behind the T7 promoter were generated and verified as described elsewhere (Svärd & Kirsebom, 1992). The various RNA molecules were generated as run-off transcription of linearized DNA plasmid using T7 DNA-dependent RNA polymerase, as described earlier (Milligan et al., 1987), with the exception that transcription was performed in the presence of 5 mM GMP and 1 mM GTP, to ensure incorporation of monophosphate at the 5′ end of the RNA (Sampson & Uhlenbeck, 1988; Wyatt et al., 1991).

To incorporate modified nucleotides into the RNA molecules, the transcription reaction was altered according to Conrad et al. (1995). Three of the unmodified NTPs and one of the corresponding modified nucleotides [dUTP (Sigma) or NTPαS (Amersham)] were added to the reaction mixture to the final concentration of 1 mM. In the transcription reactions with dUTP, $MgCl_2$ was substituted with 2.5 mM $MnCl_2$ (Conrad et al., 1995).

All RNA molecules were purified on 20% denaturing polyacrylamide gels and renatured as described (Tallsjö et al., 1996). Transcripts that needed to be 5′ end-labeled with γ-^{32}P were dephosphorylated, subsequently kinased with [γ-^{32}P]ATP, and purified according to standard procedures.

RNA molecules only partially substituted with modified nucleotides, i.e., containing modified nucleotides only in one of the halves (see Fig. 1B), were prepared by ligation of two RNA fragments according to Moore and Sharp (1992). One of the fragments contained modified nucleotides introduced as described above and the other one was fully unmodified. Prior to ligation, the 5′ fragment was kinased as described above. This reaction mixture was added to the annealing reaction together with equal amounts of the 3′ fragment and a DNA oligonucleotide template [5′-CCCGGGCCGAAGCC CCTAT], complementary to the junction region in the tetraloop, heated at 95 °C for 5 min, and subsequently put on ice. Ligation buffer containing 50 mM Tris-HCl, pH 7.5, 10 mM $MgCl_2$, 20 mM DTT, 50 μg/mL BSA, and PEG 6000 to a final concentration of 12–14% (w/v) was added together with RNA guard (Pharmacia), 1 mM ATP, and 10 units of T4 DNA ligase (Pharmacia). The reaction was allowed to proceed overnight at 16 °C and the ligated products were separated and purified as described above.

Enzymatic and chemical probing of RNA

Prior to structural probing reactions, the RNA samples were renatured in appropriate buffer by heating at 55 °C for 5 min followed by incubation at 37 °C.

Enzymatic probing was performed following protocols described previously (Ehresmann et al., 1987). Usually, approximately 1 pmol of end-labeled RNA was subjected to partial digestion by endonucleases [0.1–0.2 units of RNase T1 (Gibco-BRL), 0.01–0.2 units of RNase T2 (Gibco-BRL) or 0.0001–0.005 units of RNase V1 (Pharmacia) per reaction] in 10 μL of 50 mM Tris-HCl, pH 7.2, 100 mM NH_4Cl, 10 mM $MgCl_2$ at 37 °C. The reaction was terminated after 2 min by the addition of 2 volumes of stop solution (10 M urea, 10 mM EDTA, bromophenol blue, and xylene cyanol blue). The reactions were further analyzed on 20% denaturing polyacrylamide gels.

Chemical modifications were performed as described elsewhere (Peattie & Gilbert, 1980; Ehresmann et al., 1987). The reactions were analyzed on 20% denaturing polyacrylamide gels.

Modification with CMCT

Modification with CMCT was performed using unlabeled RNA (approximately 20 pmol) in 200 μL of 50 mM Na-borate, pH 8,

20 mM $Mg(OAc)_2$, 300 mM KCl (native conditions), or 50 mM Na-borate, pH 8, 1 mM EDTA (semi-denaturing and denaturing conditions). The reaction was initiated by the addition of 50 μL of a 70 mg/mL CMCT (Sigma) solution (freshly prepared) and was performed for 30 min at 37 °C (native and semi-denaturing conditions) or for 10 min at 90 °C (denaturing conditions). The reaction was terminated by precipitation with 2.5 volumes of 99% ethanol. Sites of modifications were identified by primer extension according to standard procedures using a primer complementary to the 3′ end of the RNA (5′-AGCCTACCCGGGCCG).

Modification with DEPC

Modification with DEPC was conducted using an end-labeled RNA (approximately 0.5 pmol) in 200 μL of 50 mM Na-cacodylate, pH 7.3, 10 mM $MgCl_2$ (native conditions) or 50 mM Na-cacodylate, pH 7.3, 1 mM EDTA (semi-denaturing and denaturing conditions). The reaction was initiated by the addition of 20 μL of DEPC (Sigma) and performed for 60–90 min at 37 °C (native and semi-denaturing conditions) or for 15 min at 90 °C (denaturing conditions). After precipitation, the samples were treated with aniline (Peattie & Gilbert, 1980).

Modification with DMS

Modification with DMS was performed in the same buffer as used for the DEPC modifications. The reaction was initiated by the addition of 0.5 μL of DMS (Sigma) and performed for 15 min at 37 °C (native and semi-denaturing conditions) or for 1 min at 90 °C (denaturing conditions), and it was terminated by the addition of 100 μL of ice-cold 0.75 M NaOAc, pH 5.5, and 0.5 M 2-mercaptoethanol followed by ethanol precipitation and aniline treatment.

Partial alkaline hydrolysis

Partial alkaline hydrolysis of RNA was conducted in 50 mM NaOH, 1 mM EDTA at 100 °C for 10–30 s and the reactions were terminated by the addition of equal volume of 10 M urea, 80 mM NaOAc, 1% acetic acid.

Metal ion-induced cleavage of the 31-mer RNA variants

Lead(II)-induced cleavage was performed as described (Ciesiolka et al., 1994; Kufel & Kirsebom, 1996). RNA was 5′ end-labeled, purified, and renatured as described above. RNA (approximately 2 pmol) was preincubated for 10 min at 37 °C in 50 mM Tris-HCl, pH 7.5, 100 mM NH_4Cl, and 10 mM $MgCl_2$. Cleavage was initiated by the addition of freshly prepared $Pb(OAc)_2$ to a final concentration of 0.1–0.25 mM. The reaction was terminated after 10–15 min by the addition of two volumes of stop solution (see above). Magnesium(II)-induced cleavage was conducted according to Kazakov and Altman (1991). The reaction mixture contained 100 mM NH_4Cl, 50 mM Ches, pH 9.5, and 10 mM $MgCl_2$. Reactions were incubated at 37 °C for 6 h and terminated by the addition of two volumes of stop solution (see above). Cleavage products were separated on a 20% denaturing polyacrylamide gel. Metal ion cleavage was also observed without ligating the two halves, however, here the results were less conclusive.

The Pb^{2+}- or Mg^{2+}-induced cleavage sites in the region of the P15 internal loop of the full-length M1 RNA were mapped by primer extension analysis using a primer complementary to positions 358–377 [AV22 (Kufel & Kirsebom, 1996)].

RNase H cleavage

The experiments were conducted as described previously (Kufel & Kirsebom, 1996). Approximately 0.2 pmol of 5′ end-labeled RNA (see above) was renatured prior to the reaction in 25 mM Tris-HCl, pH 7.9, 50 mM KCl by heating for 5 min at 55 °C followed by incubation at 33 °C for 5 min. Subsequently, 2–10 pmol of a short deoxyribooligonucleotide (either 5′-CACCCA or 5′-CAGCCA, where the underlined nucleotides are complementary to residues G23–U26 in either the wild-type 31-mer RNA or the "C293" derivative, respectively) was added and allowed to hybridize to the RNA at 33 °C for 10 min. Cleavage was performed in 25 mM Tris-HCl, pH 7.9, 50 mM KCl, 1 mM DTT at 33 °C for 30 min using 10 U of RNase H (Amersham). The reaction was terminated by the addition of two volumes of stop solution (see above). Cleavage products were separated on a 20% denaturing polyacrylamide gel.

Preparation of substrate and RNase P RNA carrying phosphothioates 3′ of G293 and cleavage assay conditions

The model substrate, pATSer, gene carried a *Pst* I site to generate the desired precursor after cleavage and transcription with T7 DNA-dependent RNA polymerase (see Fig. 5; Milligan et al., 1987). Characterization of this substrate will be described elsewhere.

To generate M1 RNA molecules carrying substitution of the Rp- and Sp-oxygens 3′ of G293, we prepared two M1 RNA fragments using T7 DNA-dependent RNA polymerase, one containing residues 1–291, and the other, residues 300–377. The remaining fragment comprising residues 292–299 with and without substitutions was chemically synthesized by Interactiva Biotechnologie GmbH, Germany. The RNA fragments were ligated using the method of Moore and Sharp (1992) as described above. The ligation efficiency was approximately 1% and ligated M1 RNA derivatives were gel purified and used as described below.

Cleavage was performed at 37 °C as we described elsewhere with the exception that we used 40 mM $MgCl_2$ (or as indicated) instead of the usual 100 mM $MgCl_2$ (see, for example, Tallsjö et al., 1996). The concentration of substrate was 7.5 nM and the enzyme concentration was approximately 20 nM. Samples were withdrawn at different time points after mixing preincubated M1 RNA with preheated substrate and stopped by adding 4.5 times the volume of warm stop solution (10 M urea, 10 mM EDTA, and bromphenol blue). The cleavage products were separated on 20% denaturing polyacrylamide gels and catalytic activity was quantified using a PhosphorImager.

Rescue experiments were performed using the following conditions: (1) 5 mM $MnCl_2$ and 35 mM $MgCl_2$; (2) 2.5 mM

$CdCl_2$ and 37.5 mM $MgCl_2$; or (3) 2.5 mM $ZnCl_2$ and 37.5 mM $MgCl_2$.

ACKNOWLEDGMENTS

We thank Dr. Eric Westhof for fruitful discussions, Dr. Hans Eklund for his assistance in generating Figure 6, and Dr. Jyoti Chattopadhyaya for discussions. Dr. Eileen Bridge is acknowledged for critical reading of the manuscript. This work was supported by grants from the Swedish Natural Science Research Council and the Swedish Research Council for Engineering Sciences to L.A.K.

Received July 2, 1997; returned for revision August 13, 1997; revised manuscript received April 3, 1998

REFERENCES

Altman S, Kirsebom LA, Talbot S. 1995. Recent studies of RNase P. In: Söll D, RajBhandary UL, eds. *tRNA structure, biosynthesis, and function*. Washington, DC: ASM Press. pp 67–78.

Bassi GS, Murchie AIH, Lilley DMJ. 1996. The ion-induced folding of the hammerhead ribozyme: Core sequence changes that perturb folding into the active conformation. *RNA 2*:756–768.

Brown JW. 1996. The ribonuclease P database. *Nucleic Acids Res 24*:236–237.

Brown RS, Dewan JC, Klug A. 1985. Crystallographic and biochemical investigation of the lead(II)-catalyzed hydrolysis of yeast phenylalanine tRNA. *Biochemistry 24*:4785–4801.

Cate JH, Doudna JA. 1996. Metal-binding sites in the major groove of a large ribozyme domain. *Structure 4*:1221–1229.

Cate JH, Gooding AR, Podell E, Zhou K, Golden BL, Kundrot CE, Cech TR, Doudna JA. 1996. Crystal structure of a group I intron ribozyme domain: Principles of RNA packing. *Science 273*:1678–1685.

Cate JH, Hanna RL, Doudna JA. 1997. A magnesium ion core at the heart of a ribozyme domain. *Nature Struct Biol 4*:553–558.

Ciesiolka J, Hardt WD, Schlegel J, Erdmann VA, Hartmann RK. 1994. Lead-ion-induced cleavage of RNase P RNA. *Eur J Biochem 219*:49–56.

Conrad F, Hanne A, Gaur RK, Krupp G. 1995. Enzymatic synthesis of 2′-modified nucleic acids: Identification of important phosphate and ribose moieties in RNase P substrates. *Nucleic Acids Res 23*:1845–1853.

Correll CC, Freeborn B, Moore PB, Steitz TA. 1997. Metals, motifs, and recognition in the crystal structure of a 5S rRNA domain. *Cell 91*:705–712.

Ehresmann C, Baudin F, Mougel M, Romby P, Ebel JP, Ehresmann B. 1987. Probing the structure of RNAs in solution. *Nucleic Acids Res 15*:9109–9128.

Easterwood TR, Harvey SC. 1997. Ribonuclease P RNA: Models of the 15/16 bulge from *Escherichia coli* and the P15 stem loop of *Bacillus subtilis*. *RNA 3*:577–585.

Glemarec C, Kufel J, Földesi A, Maltseva T, Sandström A, Kirsebom LA, Chattopadhyaya J. 1996. The NMR structure of 31mer RNA domain of *Escherichia coli* RNase P RNA using its non-uniformly deuterium labelled counterpart [the "NMR-window" concept]. *Nucleic Acids Res 24*:2022–2035.

Grasby JA, Mersmann K, Singh M, Gait MJ. 1995. Purine functional groups in essential residues of the hairpin ribozyme required for catalytic cleavage of RNA. *Biochemistry 34*:4068–4076.

Greenbaum NL, Radhakrishnan I, Hirsh D, Patel DJ. 1995. Determination of the folding topology of the SL1 RNA from *Caenorhabditis elegans* by multidimensional heteronuclear NMR. *J Mol Biol 252*:314–327.

Guerrier-Takada C, Altman S. 1984. Structure in solution of M1 RNA, the catalytic subunit of ribonuclease P from *Escherichia coli*. *Biochemistry 23*:6327–6334.

Guerrier-Takada C, Gardiner K, Marsh T, Pace N, Altman S. 1983. The RNA moiety of ribonuclease P is the catalytic subunit of the enzyme. *Cell 35*:849–857.

Holbrook SR, Sussman JL, Warrant RW, Church GM, Kim SH. 1977. RNA–ligand interactions: (I) Magnesium binding sites in yeast $tRNA^{Phe}$. *Nucleic Acids Res 4*:2811–2820.

Jack A, Ladner JE, Rhodes D, Brown RS, Klug A. 1977. A crystallographic study of metal-binding to yeast phenylalanine transfer RNA. *J Mol Biol 111*:315–328.

Jaffe EK, Cohn M. 1979. Diastereomers of the nucleoside phosphorothioates as probes of the structure of the metal nucleotide substrates and of the nucleotide binding site of yeast hexokinase. *J Biol Chem 254*:10839–10845.

Kazakov S, Altman S. 1991. Site-specific cleavage by metal ion cofactors and inhibitors of M1 RNA, the catalytic subunit of RNase P from *Escherichia coli*. *Proc Natl Acad Sci USA 88*:9193–9197.

Kirsebom LA. 1995. RNase P—A "Scarlet Pimpernel." *Mol Microbiol 17*:411–420.

Kirsebom LA, Svärd SG. 1993. Identification of a region within M1 RNA of *Escherichia coli* RNase P RNA important for the location of the cleavage site on a wild-type tRNA precursor. *J Mol Biol 231*:594–604.

Kirsebom LA, Svärd SG. 1994. Base pairing between *Escherichia coli* RNase P RNA and its substrate. *EMBO J 13*:4870–4876.

Knap AK, Wesolowski D, Altman S. 1990. Protection from chemical modifications of nucleotides in complexes of M1 RNA, the catalytic subunit of RNase P from *E. coli*, and tRNA precursors. *Biochimie 72*:779–790.

Kufel J, Kirsebom LA. 1996. Residues in *Escherichia coli* RNase P RNA important for cleavage site selection and divalent metal ion binding. *J Mol Biol 263*:685–698.

LaGrandeur TE, Hüttenhofer A, Noller HF, Pace NR. 1994. Phylogenetic comparative chemical footprint analysis of the interaction between ribonuclease P RNA and tRNA. *EMBO J 13*:3945–3952.

Milligan JF, Groebe DR, Whiterell GW, Uhlenbeck OC. 1987. Oligoribonucleotide synthesis using T7 RNA polymerase and DNA templates. *Nucleic Acids Res 15*:8783–8798.

Moore MJ, Sharp PA. 1992. Site-specific modification of pre-mRNA: The 2′ hydroxyl groups at the splice sites. *Science 256*: 992–997.

Oh BK, Pace NR. 1994. Interaction of the 3′-end of tRNA with ribonuclease P RNA. *Nucleic Acids Res 22*:4087–4094.

Pace NR, Brown JW. 1995. Evolutionary perspective on the structure and function of ribonuclease P, a ribozyme. *J Bacteriol 177*:1919–1928.

Peattie DA, Gilbert W. 1980. Chemical probes for higher-order structure in RNA. *Proc Natl Acad Sci USA 77*:4679–4682.

Pley HW, Flaherty KM, McKay DB. 1994. Three-dimensional structure of a hammerhead ribozyme. *Nature 372*:68–74.

Sampson JR, Uhlenbeck OC. 1988. Biochemical and physical characterization of an unmodified yeast phenylalanine transfer RNA transcribed in vitro. *Proc Natl Acad Sci USA 85*:1033–1037.

Schweisguth DC, Chelladurai BS, Nicholson AW, Moore PB. 1994. Structural characterization of a ribonuclease III processing signal. *Nucleic Acids Res 22*:604–612.

Scott WG, Finch JT, Klug A. 1995. The crystal structure of an all-RNA hammerhead ribozyme: A proposed mechanism for RNA catalytic cleavage. *Cell 81*:991–1002.

Scott WG, Murray JB, Arnold JRP, Stoddard BL, Klug A. 1996. Capturing the structure of a catalytic RNA intermediate: The hammerhead ribozyme. *Science 274*:2065–2069.

Shiraishi H, Shimura Y. 1988. Functional domains of the RNA component of ribonuclease P revealed by chemical probing of mutant RNAs. *EMBO J 7*:3817–3821.

Simorre JP, Legault P, Hangar AB, Michiels P, Pardi A. 1997. A conformational change in the catalytic core of the hammerhead ribozyme upon cleavage of an RNA substrate. *Biochemistry 36*:518–525.

Streicher B, Westhof E, Schroeder R. 1996. The enviroment of two metal ions surrounding the splice site of a group I intron. *EMBO J 15*:2556–2564.

Svärd SG, Kagardt U, Kirsebom LA. 1996. Phylogenetic comparative mutational analysis of the base-pairing between RNase P RNA and its substrate. *RNA 2*:463–472.

Svärd SG, Kirsebom LA. 1992. Several regions of a tRNA precursor determine the *Escherichia coli* RNase P cleavage site. *J Mol Biol 227*:1019–1031.

Tallsjö A, Kufel J, Kirsebom LA. 1996. Interaction between *Escherichia coli* RNase P and the discriminator base results in slow product release. *RNA 2*:299–307.
Westhof E, Wesolowski D, Altman S. 1996. Mapping of three dimensions of regions in a catalytic RNA protected from attack by an Fe(II)-EDTA reagent. *J Mol Biol 258*:600–613.
Wimberly B, Varani G, Tinoco I Jr. 1993. Conformation of loop E from eukaryotic 5S RNA. *Biochemistry 32*:1078–1087.
Wyatt JR, Chastain M, Puglisi JD. 1991. Synthesis and purification of large amounts of RNA oligonucleotides. *BioTechniques 11*:764–769.
Xu J, Lapham J, Crothers DM. 1996. Determining RNA solution structure by segmental isotopic labelling and NMR: Application to *Caenorhabditis elegans* spliced leader RNA 1. *Proc Natl Acad Sci USA 93*:44–48.
Zito K, Hüttenhofer A, Pace NR. 1993. Lead-catalyzed cleavage of ribonuclease P RNA as a probe for integrity of tertiary structure. *Nucleic Acids Res 21*:5916–5920.